Design of Performance Enhanced Metamaterial-Enabled Absorber for Low-Power IoT Networks

Kozhakhmet Abdugapbar, Kassen Dautov, Mohammad Hashmi, and Galymzhan Nauryzbayev(✉)

School of Engineering and Digital Sciences, Nazarbayev University, Astana 010000, Kazakhstan
{kozhakhmet.abdugapbar,kassen.dautov,mohammad.hashmi, galymzhan.nauryzbayev}@nu.edu.kz

Abstract. A single-band metamaterial absorber (MTMA) for Internet-of-Things (IoT) networks, working at 5.8 GHz, is presented. The proposed unit cell with a size of 16×16 mm^2 has circular and square rings designed on a Rogers RO4350B substrate with a thickness of 1.54 mm. The material properties of the absorber are extracted and used to show the double negative metamaterial behavior. The real and imaginary values of impedance demonstrate the matching of MTMA with the free space. Furthermore, MTMAs with various configurations are designed to validate the impact on the absorption level and operating frequency. All array configurations exhibit nearly perfect, 99.9% absorbance. The physical mechanism of MTMA is discussed using an electric field and surface current distributions. The obtained results of the study reveal that the proposed MTMA can be used to charge low-power IoT devices.

Keywords: Array · Electromagnetic waves · Internet-of-Things (IoT) · Metamaterial absorber · Unit cell

1 Introduction

Recently, the Internet-of-Things (IoT) is a rapidly evolving technology that is present in every part of industry and daily life. In general, these devices are powered by batteries, which cause high maintenance costs due to the regular replacement [1]. Since difficulties with a big size and weight are also present, an alternative sustainable powering becomes a challenge [2,3]. Radio frequency (RF) energy harvesting (EH) is one of the viable solutions because of its availability [4]. Numerous wireless technologies operate using electromagnetic (EM) waves that can be transformed into useful energy. However, the RF power density is low, between 0.2 nW/cm^2–1 μW/cm^2, therefore, an efficient absorber is needed for the EH purposes [5].

This research was funded by Nazarbayev University under Collaborative Research Program Grants #11022021CRP1513 (G. Nauryzbayev) and #021220CRP0222 (M. Hashmi).

K. Rabie et al. (Eds.): IoTaaS 2022, LNICST 506, pp. 38–47, 2023.
https://doi.org/10.1007/978-3-031-37139-4_4

Absorbers are introduced as a key enabling component of the EH-based system that scavenges energy from the radio waves. There are several energy harvester types: the high-gain antenna, the dipole antenna, the graphene-based and the metamaterial absorber (MTMA). Nowadays, MTMAs are considered an effective absorber type and attract many researchers. MTMA has extraordinary properties such as the beating diffraction limit, negative permeability (μ) and permittivity (ε) [6]. MTMA is a composite structure that has the potential to reduce the incoming EM wave reflections and, therefore, provides a variety of benefits over traditional absorbers in terms of effective size reduction, vast flexibility, and low profile.

Recently, the work on MTMAs that have high absorption levels and different operating frequencies has been reported. The design of absorbers is important due to the impact on an absorption rate, and researchers presented various unit cells (UCs) with patterns such as square, double, split rings, *etc.* For example, single-band MTMA working at 2.4 GHz had a pattern with two circular rings, the parameters of which were optimized to define the frequency and absorption level [7]. Furthermore, UCs were combined into an array that led to an increased absorption efficiency of 84.7%. Another single-band absorber was designed to have 93% absorption at 2.45 GHz [8]. Alternatively, multi-band absorbers have several resonance frequencies, which increase the amount of harvested energy. One of the examples was dual-band MTMA working at 6.46 GHz and 7.68 GHz, which showed 95% absorbance at both frequencies [9]. The design of UC was done step-by-step, first obtaining two resonance frequencies and then increasing the absorption rate by implementing another resonator. Furthermore, a triple-band split ring resonator-based absorber operating at 4.19 GHz, 6.64 GHz and 9.95 GHz had an efficiency of 97.5%, 96.5% and 98.85% [10].

This paper proposes high-absorbance MTMA working at practical ISM (industrial, scientific and medical) frequency bands used in WiFi and radio local area networks. It should be noted that effective MTMA may result in efficient RF EH and replace batteries of IoT devices. To achieve a high absorbance rate, the proposed UC geometry was thoroughly analyzed. MTMA was investigated for the presence of any metamaterial behavior and showed a double-negative nature. Then, designed UC was used to construct MTMA with various array configurations. The final absorbance rate of optimal array-type MTMA was 99.9%.

The remaining sections of this paper are organized as follows. Section. 2 discusses the step-by-step design of UC and its associated challenges. The metamaterial properties of proposed UC are extracted and discussed in Sect. 3. Furthermore, developed MTMA using UCs is presented in Sect. 4. The design of MTMA and corresponding results are concluded in Sect. 5.

2 Unit Cell Design

The effectiveness of the absorber depends on the level of absorption, which is calculated using reflected (S_{11}) and forward transmission (S_{21}) waves as

$$A(\omega) = 1 - |S_{21}| - |S_{11}|. \tag{1}$$

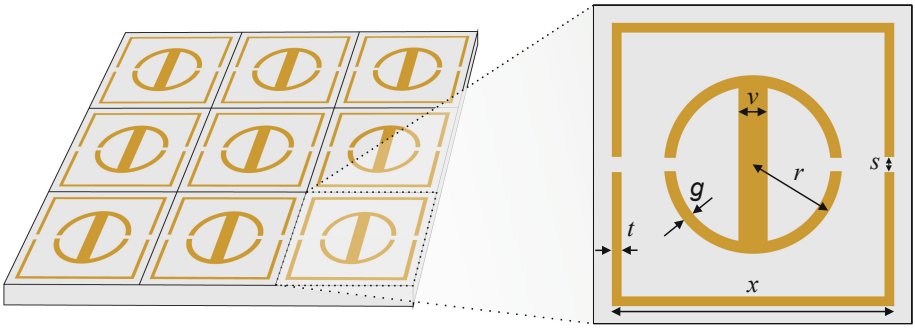

Fig. 1. The proposed UC design.

The proposed design of UC has a copper layer at the bottom of a structure, which reflects all coming waves to the incident port. As a sequence, this leads to the zero transmittance and (1) becomes as follows

$$\mathrm{A}(\omega) = 1 - |\mathrm{S}_{11}| \,. \tag{2}$$

The considered UC geometry was analyzed to identify the optimal parameters that result in superior performance. Designed UC consists of square and circular rings with a line, as presented in Fig. 1. The structure of UC consists of the dielectric material and the copper layers at the bottom and top. The thickness of the copper layers are 0.035 mm, while the Rogers RO4350B with dielectric constant 3.66 and loss tangent 0.0037, substrate's height is 1.54 mm. The parameters, which affect the performance, are the radius of the inner circular ring (r) with width (g) and the length of outer square ring (x) with width (t). Both the rectangular and circular rings have two slits with width (s) while the line in the circular ring has width (v). All the discussed parameters are analyzed to increase absorption at the intended working frequency of 5.8 GHz.

2.1 Performed Analysis

As previously discussed the parameters of UC play a major role in MTMA's performance. Changing the parameters of the proposed design affects the absorption and resonance frequencies, simultaneously, and certain parameters with a higher absorption may have different frequency than needed. The pattern of UC defines the absorption rate and bandwidth. The design is developed step-by-step, adding more complex elements. The initial design of UC consists of a square ring with gaps, as presented in Fig. 2. This design results in a single resonance frequency at a higher frequency with a low absorption rate. The second step is to add another resonator, a circular ring inside of the square one, and this modification shifted the operating frequency to 5.8 GHz. The reason of adding another resonator is that the first square is not enough to shift down the frequency further. Additionally, the last design includes a line connecting two semicircles, which

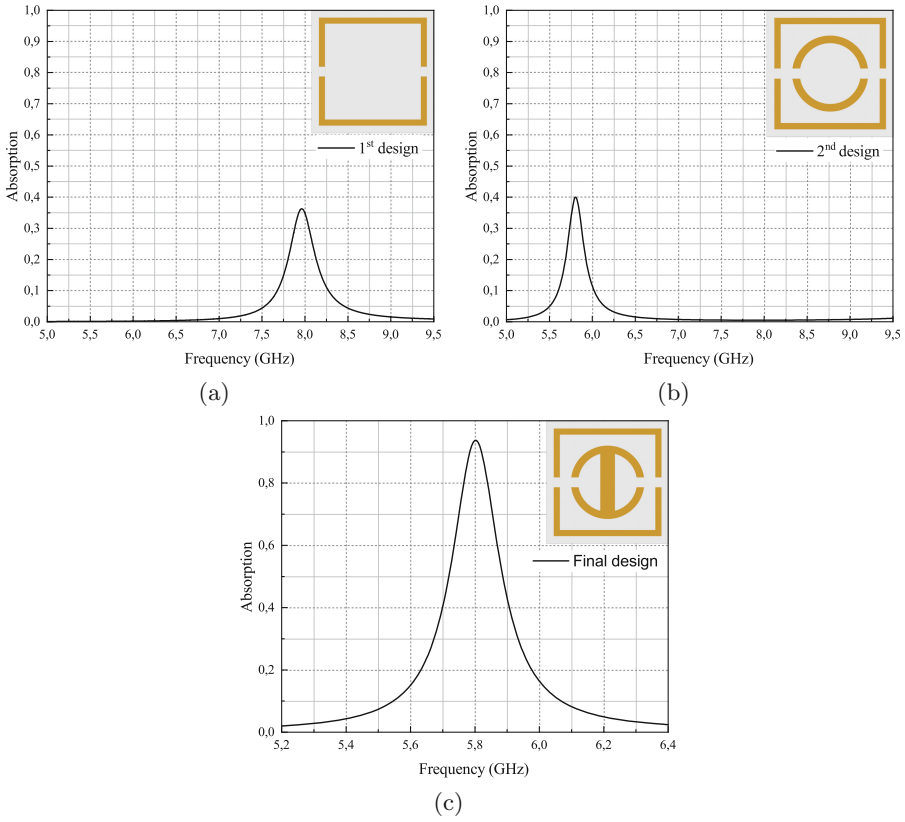

Fig. 2. The UC design steps.

significantly raises the absorption level. The performed analysis aims to find the optimal values for the highest possible absorption rate while keeping the resonance at 5.8 GHz.

The optimal UC design is obtained from completing the parametric analysis, which is done by alternating g and t. Figure 3a presents the absorbance with changing t. When the width is 0.2 mm, it reaches the high absorption rate and satisfies the needed frequency, while for higher values of t, there is a shift of the resonance frequency. Furthermore, Fig. 3b shows the absorption ratio at different values of g. It is observed that 0.4 mm width is perfect in terms of both absorbance level and frequency. On the other hand, if the width grows, the operating frequency will get higher than 5.8 GHz. From the performed analysis, the most absorbance was obtained, when $g = 0.3$ mm and $t = 0.2$ mm. The UC, with optimal parameters presented in Table 1, shows 94% absorbance as depicted in Fig. 4.

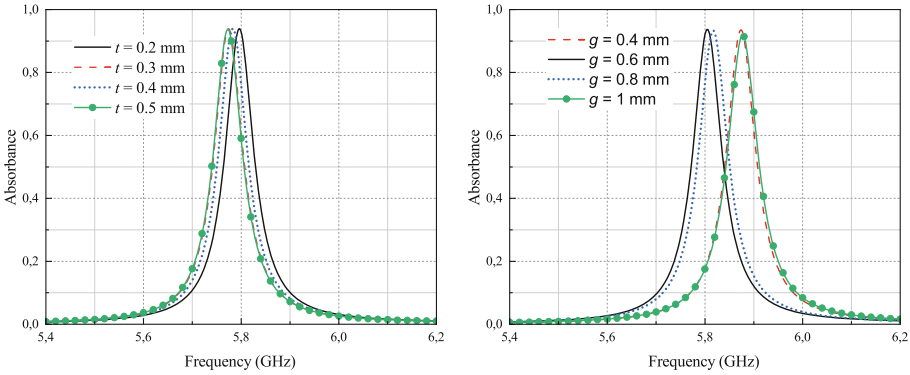

Fig. 3. Frequency vs absorption with varying: (a) t; (b) g.

Table 1. The UC parameters.

Parameter	t_{sub}	t_{cop}	r	g	t	s	x
Dimension (mm)	1.54	0.035	8	0.7	0.2	0.5	2

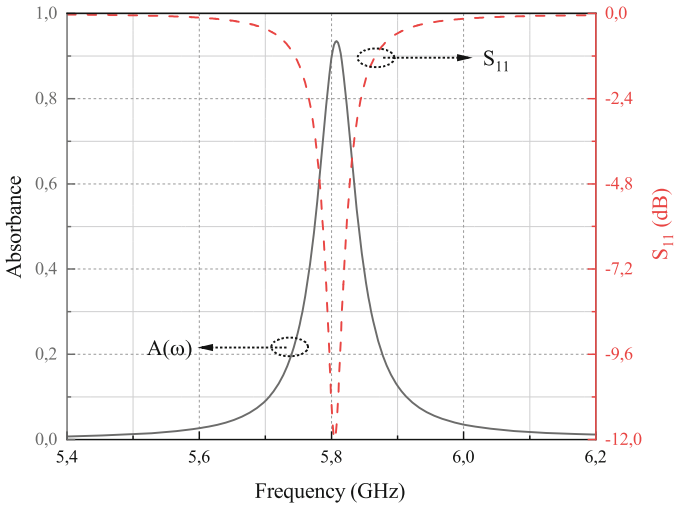

Fig. 4. The results for optimized UC.

3 Material Parameter Retrieval

For the further analysis of the MTMA behavior, the material properties (*i.e.*, ε, μ, impedance (z), refractive index (n)) of UC are extracted by using the retrieval method [12]. The S_{11} and S_{21} values are needed for obtaining the MTMA proper-

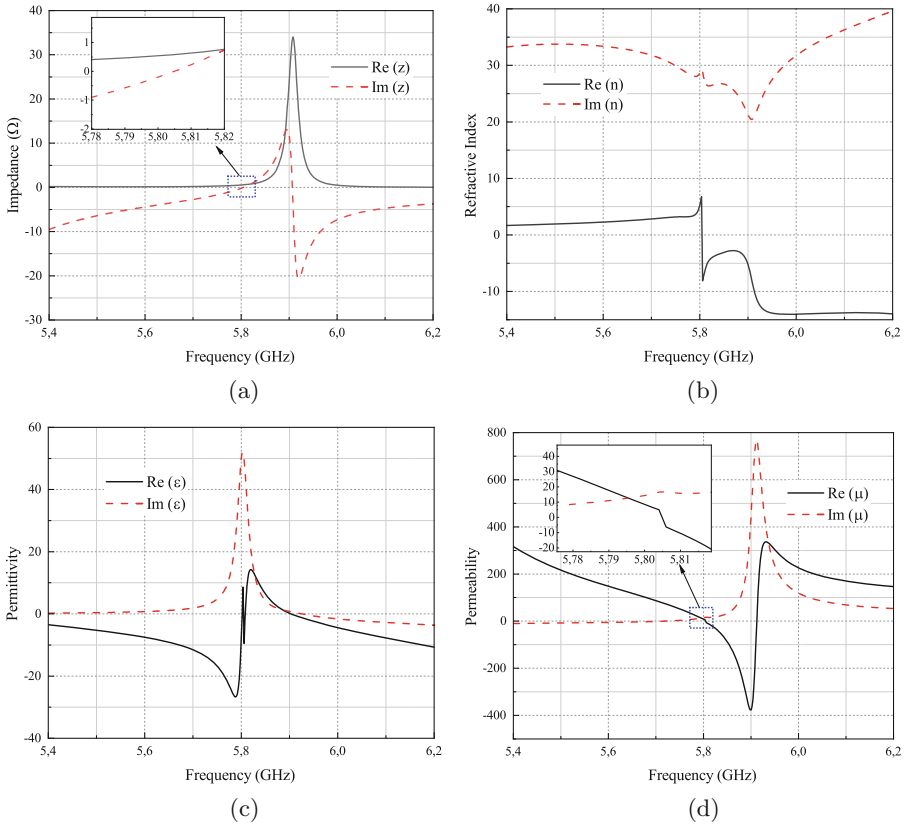

Fig. 5. Metamaterial properties: (a) z; (b) n; (c) ε; (d) μ.

ties. At the bottom layer, three holes were etched to allow waves to pass through and obtain the S_{21} values for the ε and μ calculations. These holes are small and have no impact on the absorption or resonance frequency. The scattering parameters can be described by the equations below

$$S_{11} = \frac{R_{01}\left(1 - e^{i2nk_0l}\right)}{1 - R_{01}^2 e^{i2nk_0l}}, \tag{3}$$

$$S_{21} = \frac{\left(1 - R_{01}^2\right)e^{i2nk_0l}}{1 - R_{01}^2 e^{i2nk_0l}}. \tag{4}$$

The method of the extracting metamaterial properties with S_{11} and S_{21} values comes from inverting (3) and (4) and obtaining z and n.

$$z = \sqrt{\frac{(1+S_{11})^2 - S_{21}^2}{(1-S_{11})^2 - S_{21}^2}}, \tag{5}$$

$$n = \frac{1}{k_0 l}\left[\left(\left[ln\left(e^{ink_0l}\right)\right]'' + 2m\pi\right) - i\left[\left[ln\left(e^{ink_0l}\right)\right]'\right]\right], \tag{6}$$

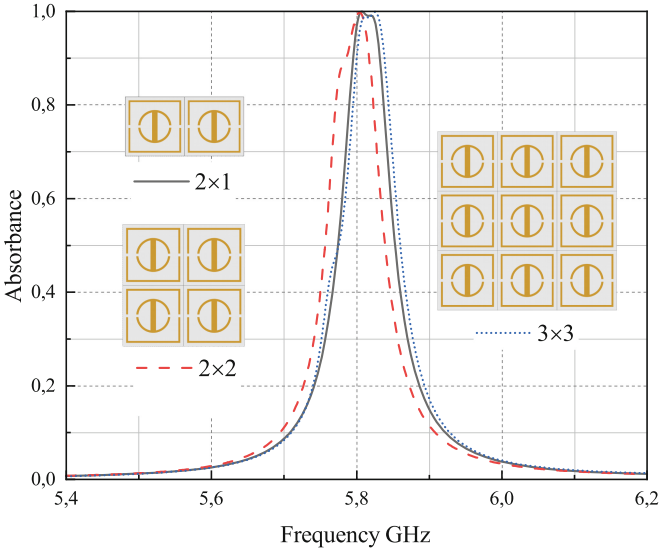

Fig. 6. Absorbance of MTMA with different configurations.

where k_0 is the wavenumber, l is the length of UC and m is the branch of periodicity. Relation of ε and μ to z and n by expressions below

$$\varepsilon = \frac{\mathrm{n}}{\mathrm{z}}, \tag{7}$$

$$\mu = \mathrm{nz}. \tag{8}$$

The functions of ε and μ are complex and need analysis to identify the metamaterial nature of UC.

Figure 5 depicts the material properties calculated using (5)–(8) with the S_{11} and S_{21} values. The value of real impedance reaches 1 Ω and the imaginary part is close to 0 Ω at the resonance frequency, as shown in Fig. 5a, which indicates the impedance matching between the absorber and free space [13]. Figure 5b shows that the real part of the refractive index is negative at 5.8 GHz. The positive impedance and the negative refractive index at the resonance frequency represent the metamaterial behavior of UC.

The metamaterials are divided into four types depending on the values of μ and ε which determine the metamaterial behavior [14]. There are three types of medium: *double − positive medium*, when both μ and ε are positive; *epsilon − negative medium*, where only ε is negative, *mu − negative medium*, where μ is lower than zero; and *double − negative medium*, where both parameters are below zero. Figures 5c and 5d show that the real parts of μ and ε at 5.8 GHz are −10 and −8, respectively. The negative values of μ and ε define the double-negative metamaterial property. Furthermore, the plots of refractive index, permeability, and permittivity demonstrate an incline from positive to

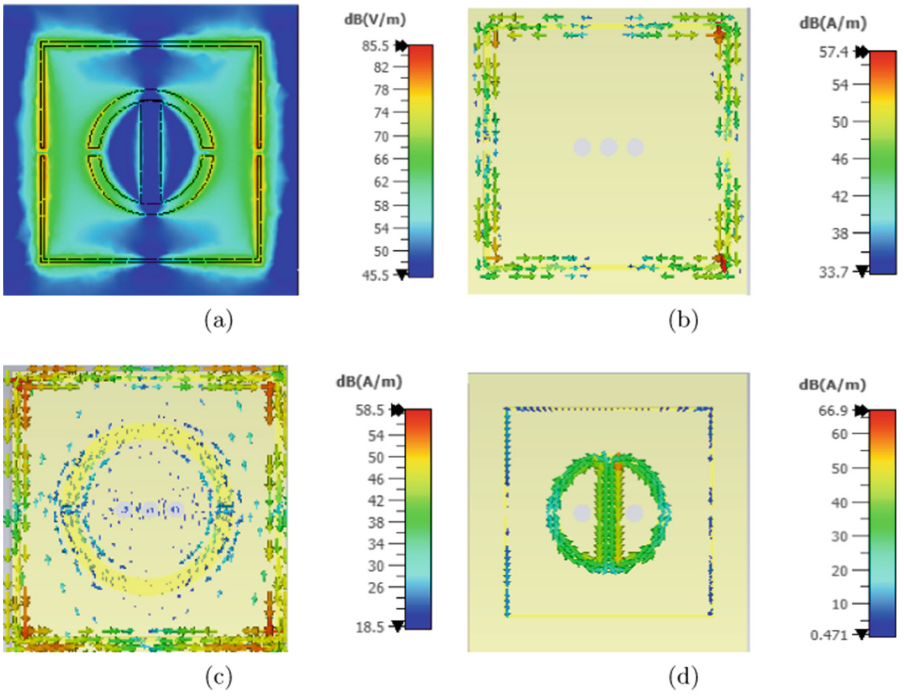

Fig. 7. (a) The electric field distribution; (b) The surface current of 1st design; (c) The surface current of 2nd design; (d) The surface current of final design;

negative values at 5.8 GHz. It is worth noting that this phenomenon appears with only artificial metamaterial devices. All these prove that proposed UC has metamaterial properties.

4 Metamaterial-Based Absorber Development

The size of IoT devices is different, which varies from small-sized to huge sensors. It is important to examine the impact of an array size on the frequency and absorption, since the possibility to change the array size without a major shift in the frequency and absorption loss, gives wider coverage area and, therefore, more harvested energy. Designed UC is used to construct the arrays of 2×1, 2×2, and 3×3, as shown in the inset of Fig. 6.

It is imperative to note that all three array-based MTMAs demonstrated 99.9% absorption. The array size has a negligible impact on the frequency shift and increases the absorption rate, making it nearly perfect. The slight changes in the frequency may be caused by the mutual coupling between adjacent UCs. The presented MTMA's efficiency is capable of powering small devices and sensors. It is compact and can be attached to most small sensors and can be used to cover large areas without a shift in the resonance frequency. The electric field

Table 2. The UC parameters.

Ref	UC size, mm^2	Frequency, GHz	Absorbance, %	UC thickness, mm	Application
[7]	50×50	2.4	88.5	1	Radio wave absorber
[9]	35×35	6.46 / 7.68	95	1.6	Multi-functional sensors
[10]	14×14	4.19 / 6.64 9.95	97.5 / 96.5 98.85	1.6	Stealth technology, radar applications
[15]	20×20	2.25	99	0.5	EH
[16]	10×10	3.5	98.5	1.6	Radar cross section, antenna reduction
This work	$\mathbf{16 \times 16}$	**5.8**	**99.9**	**1.61**	**EH for IoT devices**

distribution and the surface currents of MTMA at 5.8 GHz are analyzed and presented in Fig. 7 to observe the physical characteristics. The electric field distribution is mainly concentrated near the gaps of a square ring. Therefore, the gaps in UC design are important for contributing to greater absorption. The first design of UC has surface current around the square resonator. When the second resonator is added, the surface current is present near the inner circle. In Fig 7d, where the current density of the final UC design is depicted, the surface current distribution is dense around the inner circle and line, increasing absorption rate. Table 2 shows the comparison of the previous work with proposed MTMA. Although the absorber with 10×10 mm^2 has a smaller area, the absorbance level is lower compared to [16]. It can be referred that the absorbance rate of this work is higher and the UC size is smaller. These features make the proposed design an effective EH method for low-power IoT networks.

5 Conclusion

Single-band MTMA for RF EH has been designed and analyzed in this paper. MTMAs with different configurations, constructed from proposed UCs, show a high absorption of 99.9% at 5.8 GHz. From the analysis of metamaterial behavior, MTMA has double-negative medium characteristics. The metamaterial properties and insensitivity of frequency to the array configurations make proposed MTMA suitable for EH to power IoT devices. The number of UCs may be set to any necessary value and used to cover different surface areas.

References

1. Dautov, K., et al.: Quantifying the impact of slow wave factor on closed-loop defect-based WPT systems. IEEE Trans. Instrum. Meas. **71**, 1–10 (2022)
2. Quy, V.K., et al.: IoT-enabled smart agriculture: architecture, applications, and challenges. Appl. Sci. (2076-3417), **12**(7), 3396 (2022)
3. Nauryzbayev, G., et al.: On the performance analysis of WPT-based dual-hop AF relaying networks in α - μ fading. IEEE Access **6**, 37138–37149 (2018)
4. Altinel, D., Kurt, G.K.: Modeling of multiple energy sources for hybrid energy harvesting IoT systems. IEEE Internet Things J. **6**, 10846–10854 (2019)
5. Arzykulov, S., et al.: On the capacity of wireless powered cognitive relay network with interference alignment. IEEE Glob. Commun. Conf. 1–6 (2018)

6. Dautov, K., et al.: Assessment of compact digital metasurface with beam control for WBAN applications. In: EuMC. pp. 151–154 (2022)
7. Manohar, R., Joseph, S., Ratheesh, R.: An efficient metamaterial radio wave absorber for 2.4GHz ISM band. In: 2018 3rd IEEE International Conference on Intelligent Computer Communication and Processing, pp. 648–651 (2018)
8. Xu, P., et al.: Design of an effective energy receiving adapter for microwave wireless power transmission application. In: AIP Advances. p. 6 (2016). https://doi.org/10.1063/1.4966050
9. Bakir, M., et al.: Microwave metamaterial absorber for sensing applications. Opto-Electron. Rev. **25**(4), 318–325 (2017)
10. Singh, A.K., et al.: Dual- and triple-band polarization insensitive ultrathin conformal metamaterial absorbers with wide angular stability. IEEE Trans. Electromagn. Compat. **61**(3), 878–886 (2019)
11. Wei, Y., et al.: A multiband, polarization-controlled metasurface absorber for electromagnetic energy harvesting and wireless power transfer. IEEE Trans. Microw. Theory. Tech. **70**(5), 2861–2871 (2022)
12. Chen, X., et al.: Robust method to retrieve the constitutive effective parameters of metamaterials. Phys. Rev. E - Stat. Nonlinear Soft Matter Phys. **70**(1 2), 016608-1–016608-7 (2004)
13. Paul, J.J., et al.: Compact triple-band metamaterial absorber for RF energy harvesting. In: 2020 IEEE 4th Conference on Information and Communication Technology, pp. 1–6 (2020)
14. Ma, Y., et al.: Miniaturized and dual-band metamaterial absorber with fractal Sierpinski structure. J. Opt. Soc. Am. B **31**, 325–331 (2014)
15. Amin, M., et al.: An interference-based quadruple-L cross metasurface absorber for RF energy harvesting. IEEE Antennas Wirel. Propag. Lett. **20**(10), 2043–2047 (2021)
16. Garg, P., Jain, P.: Analysis of a novel metamaterial absorber using equivalent circuit model operating at 3.5 GHz. In: 2020 IEEE International Conference on the Computation of Electromagnetic, pp. 246–247 (2020)